Applied Physics Letters

RESEARCH ARTICLE | MAY 07 2024

Modulation of dielectric properties of hexagonal/cubic boron nitride composites

Mingfei Xu ; Ziyi He ; Abhijit Biswas ; Shisong Luo ; Tao Li ; Cheng Chang ; Chenxi Li; Bin Gao ; Robert Vajtai ; Pengcheng Dai; Pulickel M. Ajayan ; Yuji Zhao

Appl. Phys. Lett. 124, 192903 (2024)
https://doi.org/10.1063/5.0210915

AIP Publishing

Applied Physics Letters ARTICLE pubs.aip.org/aip/apl

Modulation of dielectric properties of hexagonal/cubic boron nitride composites

Cite as: Appl. Phys. Lett. **124**, 192903 (2024); doi: 10.1063/5.0210915
Submitted: 27 March 2024 · Accepted: 27 April 2024 ·
Published Online: 7 May 2024

Mingfei Xu,[1] Ziyi He,[2] Abhijit Biswas,[3,a)] Shisong Luo,[1] Tao Li,[1] Cheng Chang,[1] Chenxi Li,[3] Bin Gao,[4] Robert Vajtai,[3] Pengcheng Dai,[4] Pulickel M. Ajayan,[3,a)] and Yuji Zhao[1,a)]

AFFILIATIONS

[1]Department of Electrical and Computer Engineering, Rice University, Houston, Texas 77005, USA
[2]School of Electrical, Computer, and Energy Engineering, Arizona State University, Tempe, Arizona 85287, USA
[3]Department of Materials Science and Nanoengineering, Rice University, Houston, Texas 77005, USA
[4]Department of Physics and Astronomy, Rice University, Houston, Texas 77005, USA

[a)]**Authors to whom correspondence should be addressed:** 01abhijit@gmail.com; ajayan@rice.edu; and yuji.zhao@rice.edu

ABSTRACT

In this work, we synthesized mixed-phase hexagonal-boron nitride (h-BN)/cubic-BN (c-BN) composites with varying ratios and investigated their frequency and temperature-dependent dielectric properties. As the ratio of c-BN increased, we observed a corresponding increase in the dielectric constant of the composites. Furthermore, we used spark-plasma sintering (SPS) to treat the mixed-phase composite, which resulted in a phase transformation from mixed phase to pure h-BN phase. Remarkably, the composite exhibited an increase in dielectric constant after the SPS process, which can be attributed to the densification of the composite and the enhancement in grain size. Our approach presents a promising strategy for effectively modulating the dielectric properties of BN, which is crucial for advanced electronics.

With the rapid development of modern electronic technology, there is an increasing demand for novel dielectric materials with multifunctional properties, including high dielectric constant, low dielectric loss, strong mechanical robustness, and excellent thermal conductivity.[1–7] The importance of high dielectric constant materials in electronics lies in their ability to enhance device performance, enable miniaturization, improve energy efficiency, and facilitate the development of advanced electronic systems and technologies. Ultrawide-bandgap (UWBG) material boron nitride (BN), one of the most fascinating materials, has the potential to meet these needs due to its unique structural, mechanical, electrical, optical, thermal, and chemical properties.[8–12]

Several polymorphs of BN exist, including 2D hexagonal BN (h-BN), 3D cubic BN (c-BN), wurtzite BN (w-BN), and rhombohedral BN (r-BN) phases. Among these polymorphs, 2D h-BN and 3D c-BN are the two most valuable and applicable phases, which have been widely investigated.[12] h-BN is a layered structural material with various attractive properties, including a UWBG of ∼6 eV, a high breakdown electric field of ∼10 MV/cm, a dielectric constant of ∼3.76, and a high thermal conductivity of ∼550 W/(m·K).[10,13–15] However, the relatively low dielectric constant of h-BN limits its application as a dielectric material in modern electronics and energy storage devices. Hence, it is crucial to present a feasible solution to enhance the dielectric performance of h-BN.

On the other hand, c-BN exhibits excellent dielectric, thermal, and mechanical performance.[16–20] Benefiting from its ultrawide bandgap of ∼6.4 eV, a higher dielectric constant of ∼8, a high thermal conductivity of ∼1300 W/(m·K), and strong mechanical robustness, c-BN could be used to modulate the dielectric properties of h-BN by making h-BN/c-BN nanocomposites. The combination of h-BN and c-BN could lead to synergistic effects, where the properties of the composite are superior to the individual components.[21–23]

In this paper, we synthesized h-BN/c-BN composites with different ratios and investigated their frequency and temperature-dependent dielectric properties, showing systematic variation in dielectric behaviors. Furthermore, we treated a h-BN/c-BN mixed-phase composite with spark-plasma sintering (SPS), transforming it into a pure h-BN composite. Remarkably, after the SPS treatment, the composite showed an increased dielectric constant compared to the dielectric constant of the pure h-BN composite. These observations are vital for the design and engineering of BN as a dielectric material for various applications.

We first prepared h-BN/c-BN composites and performed comprehensive structural characterizations. For synthesis, as-purchased h-BN and c-BN powders (from MSE suppliers, USA) were grounded

in an agate mortar and pestled for ~30 min by adding a few drops of polyvinyl alcohol (PVA) binder. The powders were then pressed with 4 ton load to form a compact 1-in. diameter pellet. The as-made pellet was then sealed inside a quartz tube (in vacuum) and sintered at 1000 °C for 12 h. The ramping up and down rate of the temperature was ~100 °C/h. We prepared three h-BN/c-BN composites with different ratios, including h-BN (100% molar ratio)/c-BN (0% molar ratio) [h-BN (100)/c-BN (0)] composite, h-BN (75% molar ratio)/c-BN (25% molar ratio) [h-BN (75)/c-BN (25)] composite, and h-BN (50% molar ratio)/c-BN (50% molar ratio) [h-BN (50)/c-BN (50)] composite. The area and the thickness of all three composites are ~5.07 cm^2 and ~4.9 mm, respectively.

For the h-BN (75)/c-BN (25) composite, we performed x-ray diffraction (XRD) by using the Rigaku SmartLab x-ray diffractometer (Tokyo, Japan) with a monochromatic Cu Kα radiation source ($\lambda = 1.5406$ Å). XRD pattern showed the presence of two strongest (002) peak and (111) peak (along with other Bragg peaks) that corresponded to the most stable planes of h-BN and c-BN, respectively, as shown in Fig. 1(a). Raman spectroscopy was carried out by using Renishaw via confocal microscope with a 532 nm laser as the excitation source. As shown in Fig. 1(b), the Raman spectroscopy showed a peak at ~1366 cm^{-1} that corresponded to the E_{2g} phonon mode of h-BN, while another hump at ~1054 cm^{-1} corresponded to the longitudinal optical (LO) vibrational mode of c-BN.[24,25] The origin of the strong fluorescence background observed in the Raman spectra could be due to the large background contributed by the c-BN phase.[26] Figure 1(c) shows the Fourier transform infrared spectroscopy (FTIR) obtained by using a Nicolet 380 FTIR spectrometer with a single-crystal diamond window, which clearly showed the presence of both h-BN and c-BN peaks.[27,28] Figure 1(d) shows the morphology of the composites, which was examined by using a field emission scanning electron microscope (FESEM) (FEI Quanta 400 ESEM FEG system). For FESEM, we sputtered ~10 nm gold on the surface to avoid the charging effect. FESEM clearly showed the sheet-like structure for h-BN with a grain size of ~1–2 μm and particle-like structure for c-BN with a grain size of less than 1 μm.

To investigate the dielectric properties, we performed frequency-dependent and temperature-dependent dielectric measurements on the composites. Silver paste was coated on both sides of the composites to serve as electrodes. The frequency-dependent and temperature-dependent capacitance measurements were performed using Keysight B1500A semiconductor device parameter analyzer from 5 to 800 kHz at room temperature. ε', the real part of the complex dielectric constant of the composites, can be extracted using the formula:[29]

$$\varepsilon' = \frac{C \cdot d}{\varepsilon_0 \cdot A},$$

where C is the capacitance, d is the thickness of the composites, ε_0 is the permittivity of free space, and A is the surface area of the composites. The loss tangent $\tan\delta$ can be calculated by[29]

$$\tan\delta = \frac{\varepsilon''}{\varepsilon'},$$

$$\varepsilon'' = \frac{G \cdot d}{2\pi f \cdot A},$$

where ε'' is the imaginary part of the complex dielectric constant, G is the conductance, and f is the frequency.

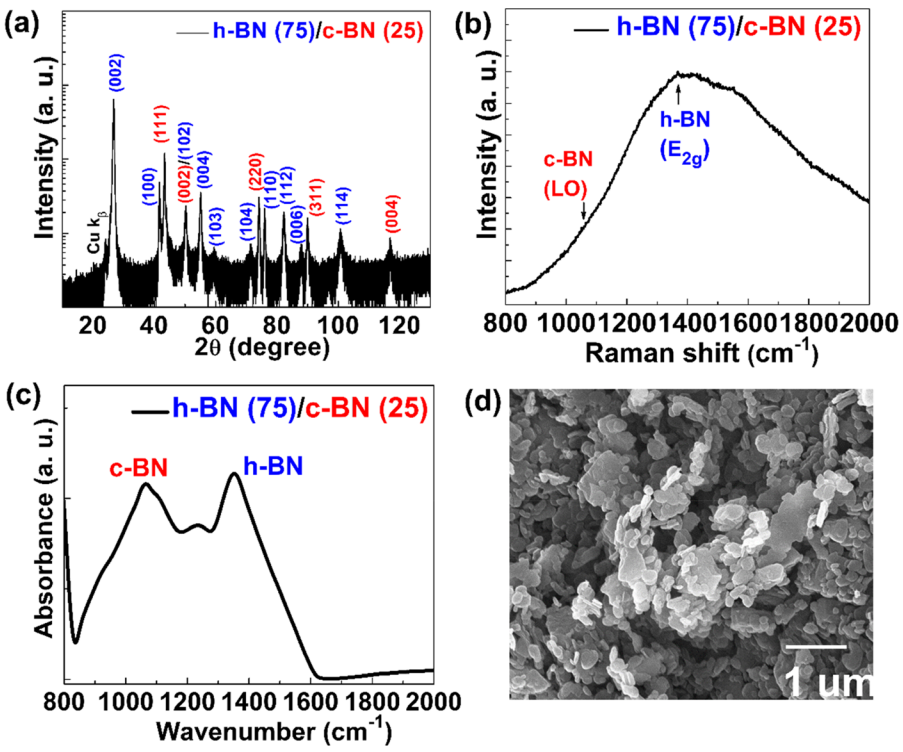

FIG. 1. Structural characterization of h-BN (75)/c-BN (25) composite. (a) XRD pattern, (b) Raman spectroscopy, (c) FTIR spectroscopy, and (d) FESEM image showing the formation of the mixed-phase composite.

For all three BN composites, the ε' has a clear decreasing trend with increasing frequencies, which is commonly observed for other dielectric materials, as shown in Fig. 2(a).[30,31] The trend can be explained by the incapability of dipoles to follow the change of the electric field at high frequencies. The ε' of h-BN (100)/c-BN (0) composite was calculated to be ~3.45 at 800 kHz and increased to ~4.11 at 5 kHz. The dielectric constant of the composites at a fixed frequency showed an increase with increasing c-BN ratio (e.g., the dielectric constant of h-BN (100)/c-BN (0) composite, h-BN (75)/c-BN (25) composite, and h-BN (50)/c-BN (50) composite at 5 kHz was ~4.11, ~4.59, and ~5.13, respectively), owing to the higher dielectric constant of c-BN and the increased interfacial polarization. Furthermore, for our composites, we did not see any trace of amorphous-BN (a-BN) phase,[26] and it has been reported that a-BN showed an ultra-low dielectric constant of ~1.30 at 800 kHz,[32] whereas our crystalline phase composites showed much higher dielectric constant values. Therefore, the existence of a-BN in our composites can be excluded. From Fig. 2(b), we could observe that all three composites had low $\tan\delta$ below 0.12, while $\tan\delta$ increased with an increasing c-BN ratio at a fixed frequency. The increase in $\tan\delta$ with an increasing c-BN ratio could be attributed to the increased interfacial polarization as h-BN and c-BN have different polarity and conductivity.[33]

We also investigated the temperature-dependent dielectric behaviors of the composites, as shown in Figs. 2(c) and 2(d). The dielectric properties of the three composites were measured at 100 kHz from 25 to 150 °C. ε' of all three composites increased with increasing temperatures, which can be attributed to enhanced interfacial polarization at higher temperatures.[34,35] $\tan\delta$ of the h-BN (100)/c-BN (0) composite had negligible dependence on temperature, while $\tan\delta$ of the h-BN (75)/c-BN (25) and the h-BN (50)/c-BN (50) composites showed a clear decreasing trend with increasing temperature. This might be attributed to the fact that the $\tan\delta$ of the mixed-phase composites is dominated by interfacial polarization, and the decreasing trend at higher temperatures is due to the space charge response, which is also observed in other materials.[36]

Furthermore, we used SPS to treat the h-BN (50)/c-BN (50) composite at 1700 °C and 90 MPa, for 1 h. The HTHP self-densification SPS process was conducted utilizing an SPS 25–10 machine from Thermal Technology LLC, California, USA, at a consistent uniaxial pressing pressure of 90 MPa and a heating rate of 50 °C/min, performed at the SPS facility in Texas A&M University, USA. The sintering temperature was maintained at 1700 °C. The sintering process followed this protocol: a mixture of h-BN and c-BN powders was placed into a graphite mold with a diameter of 1 in. and was then introduced into the sintering chamber under an initial pressure of 5 MPa. The chamber was held at $\sim 2 \times 10^{-5}$ Torr for ~30 min before sintering for 1 h under atmospheric pressure and within an ultra-high purity 5 N (~99.999%) Argon gas environment. The temperature during the SPS was monitored by using an optical pyrometer from Raytek, Berlin, Germany (model D-13127). Following the SPS process, the chamber pressure was gradually released at a rate of approximately 5 MPa/min, while the temperature was reduced at a rate of ~100 °C/min.

After the SPS process, we found that the original h-BN (50)/c-BN (50) composite was fully transformed into a pure h-BN composite (we then referred to it as the SPS h-BN composite). The area and thickness of the SPS h-BN composite are ~5.07 cm^2 and ~3.8 mm, respectively. The details of the c-BN to h-BN phase transformation using SPS have been shown in our recent studies.[26,37] Figure 3 shows the structural characterizations of the composite before and after the SPS process. Figures 3(a) and 3(e) show the XRD results of the composites. Before the SPS process, all the XRD peaks corresponding to h-BN and c-BN could be observed. In contrast, after the SPS process, only peaks corresponding to h-BN could be observed. Figures 3(b) and 3(f) show the

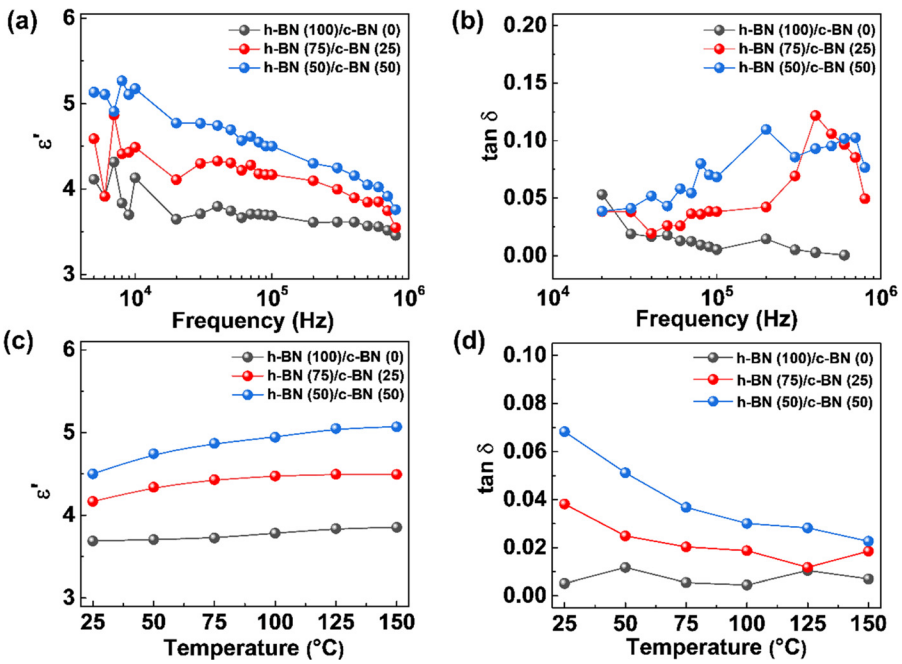

FIG. 2. (a) and (b) Frequency-dependence, and (c) and (d) temperature-dependence of dielectric constant and dielectric loss for the three BN composites.

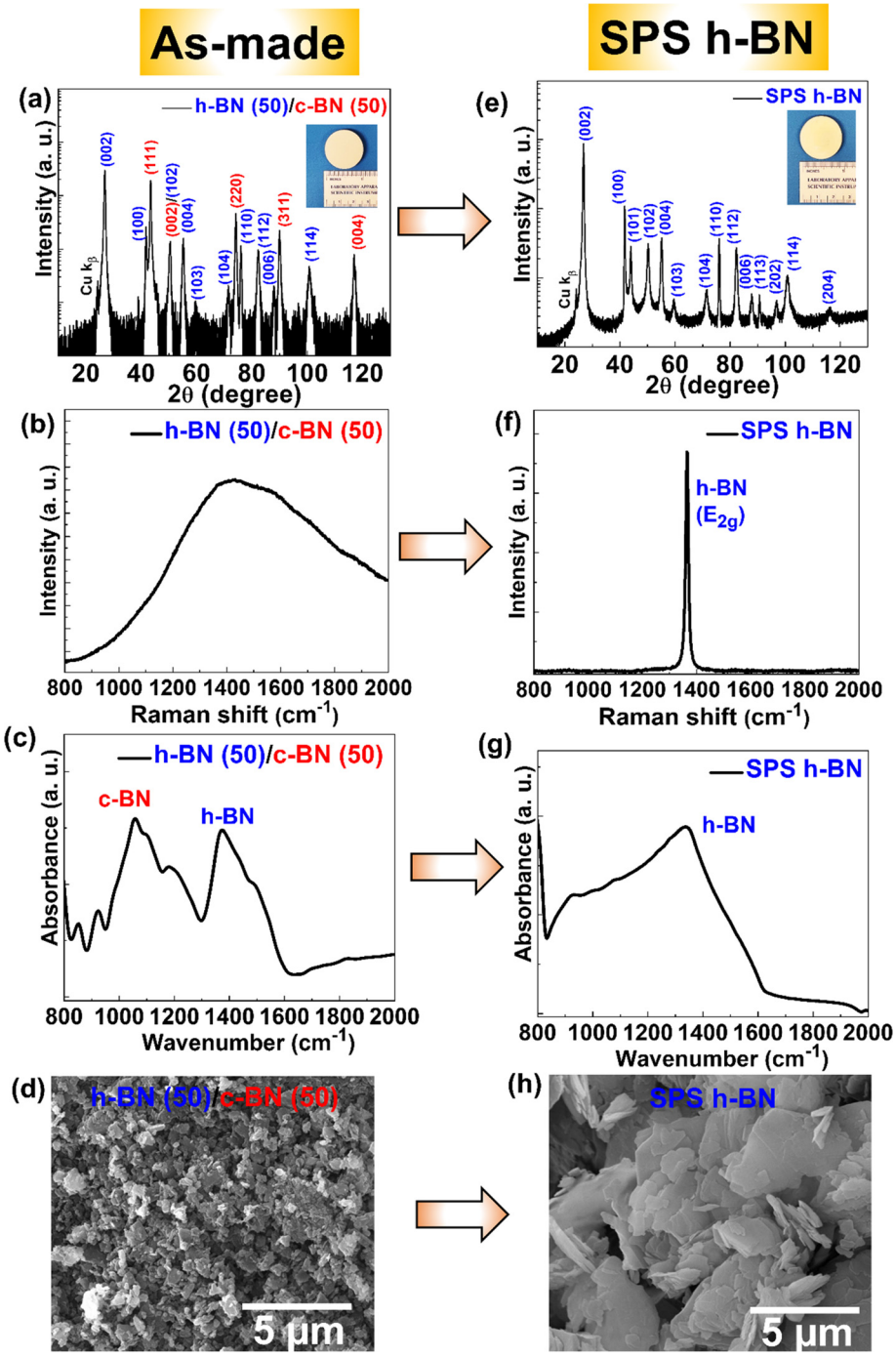

FIG. 3. Structural characterization comparison of the h-BN (50)/c-BN (50) composite and the SPS h-BN composite. (a) and (e) XRD patterns, (b) and (f) Raman spectroscopy, (c) and (g) FTIR spectroscopy, and (d) and (h) FESEM images.

Raman spectroscopy of the composites. Before the SPS process, a broad peak containing both h-BN and c-BN peaks could be observed. On the contrary, a sharp peak corresponding to h-BN could be observed after the SPS process. Figures 3(c) and 3(g) display the FTIR spectroscopy of the composites. Similarly, both h-BN and c-BN peaks could be observed before the SPS process, while only h-BN peaks could be observed after the SPS process. From FESEM, we could find both h-BN and c-BN grains before the SPS process, whereas only large h-BN sheets could be observed after the SPS process. Moreover, the density of the SPS h-BN composite increased from ∼1.35 g/cm^3 for the h-BN (100)/c-BN (0) composite to ∼2.0 g/cm^3. These results confirmed the phase

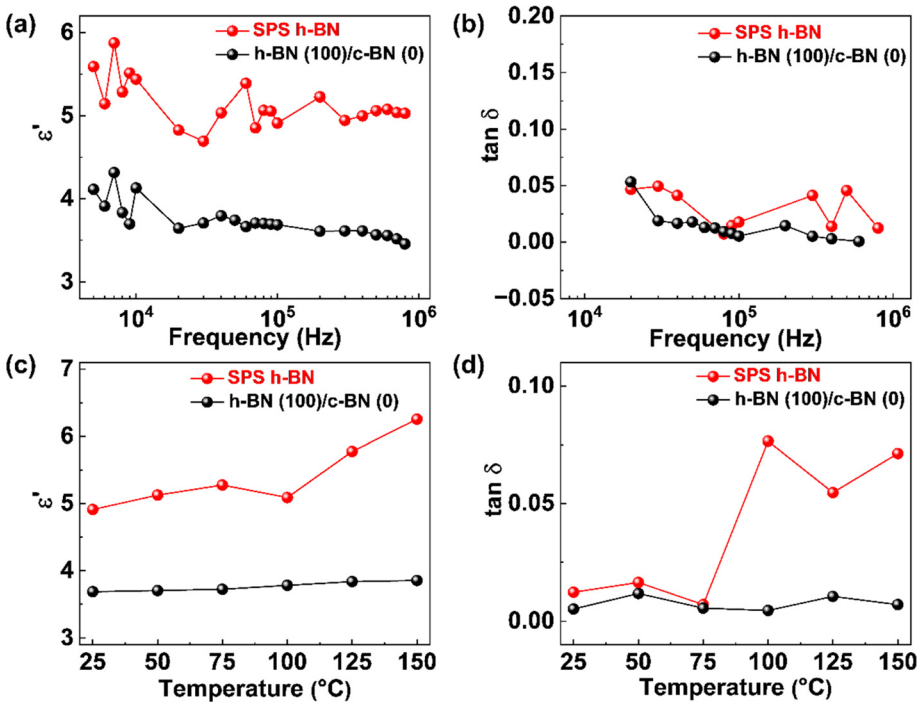

FIG. 4. Frequency-dependence of (a) dielectric constant and (b) dielectric loss, and temperature-dependence of (c) dielectric constant and (d) dielectric loss for the SPS h-BN composite and the h-BN (100)/c-BN (0) composite.

transformation from the mixed phase to the pure and high-quality h-BN phase by the SPS process.

We then measured the frequency-dependent and temperature-dependent dielectric behaviors of the SPS h-BN composite. Surprisingly, compared to the ε' at 5 kHz (4.11) of the h-BN (100)/c-BN (0) pellet, the ε' at 5 kHz of the SPS h-BN composite increased to 5.59, as shown in Fig. 4(a). The increase in ε' could be attributed to the densification of the composite and the improved grain orientation. The densification of the composite and improved orientation could increase the overall polarization and result in a higher dielectric constant. The detailed structural characterization comparison of the h-BN (100)/c-BN (0) composite and the SPS h-BN composite is included in the supplementary material. The tan δ of the SPS h-BN composite was also higher than the tan δ of the h-BN (100)/c-BN (0) composite, possibly due to the increased conduction loss, as shown in Fig. 4(b).[38,39] From Figs. 4(c) and 4(d), we could observe that ε' and tan δ of the SPS h-BN composite both show an increasing trend with increasing temperature, as conductivity and the related conduction loss would increase at higher temperatures.

In summary, we prepared h-BN/c-BN composites with different ratios using solid-state synthesis and performed frequency and temperature-dependent dielectric measurements. The dielectric constant of the composites was found to be increased with an increasing c-BN ratio. Furthermore, we treated the h-BN (50)/c-BN (50) composite with SPS, transforming the composite into a pure h-BN composite. The dielectric constant of the SPS h-BN composite showed a higher value than that of the h-BN (100)/c-BN (0) composite, attributed to the densification of the composite, the increase in grain size, and the improved grain orientation. Our work could serve as a guideline to design and engineer dielectric materials based on polymorphs of BN materials.

See the supplementary material for the frequency-dependence of capacitance and conductance for the four BN composites in Fig. S1 and for the structural characterization comparison of the h-BN (100)/c-BN (0) composite and the SPS h-BN composite in Fig. S2.

This work was supported as part of ULTRA, an Energy Frontier Research Center funded by the U.S. Department of Energy (DOE), Office of Science, Basic Energy Sciences (BES), under Award No. DE-SC0021230. This work was also supported in part by CHIMES, one of the seven centers in JUMP 2.0, a Semiconductor Research Corporation (SRC) program sponsored by DARPA.

This work was sponsored partly by the Army Research Office and was accomplished under Cooperative Agreement No. W911NF-19-2-0269. The views and conclusions contained in this document are those of the authors and should not be interpreted as representing the official policies, either expressed or implied, of the Army Research Office or the U.S. Government. The U.S. Government is authorized to reproduce and distribute reprints for Government purposes notwithstanding any copyright notation herein.

A. Biswas would also like to acknowledge to SPS facility at Texas A&M University, TX, USA. P. Dai acknowledges the materials synthesis efforts at Rice, which is supported by the U.S. DOE, BES, under Grant No. DE-SC0012311.

AUTHOR DECLARATIONS

Conflict of Interest

The authors have no conflicts to disclose.

Author Contributions

Mingfei Xu and Ziyi He contributed equally to this paper.

Mingfei Xu: Conceptualization (equal); Data curation (equal); Formal analysis (equal); Investigation (equal); Methodology (equal); Resources (equal); Software (equal); Validation (equal); Visualization (equal); Writing – original draft (lead); Writing – review & editing (lead). **Ziyi He:** Data curation (equal); Formal analysis (equal); Investigation (equal); Resources (equal); Software (equal); Validation (equal). **Abhijit Biswas:** Conceptualization (equal); Data curation (equal); Formal analysis (equal); Investigation (equal); Methodology (equal); Resources (equal); Software (equal); Supervision (equal); Validation (equal); Visualization (equal); Writing – original draft (lead); Writing – review & editing (lead). **Shisong Luo:** Conceptualization (supporting); Investigation (supporting); Methodology (supporting); Writing – original draft (supporting). **Tao Li:** Conceptualization (supporting); Investigation (supporting); Methodology (supporting); Validation (supporting). **Cheng Chang:** Conceptualization (supporting); Investigation (supporting); Methodology (supporting); Validation (supporting). **Chenxi Li:** Conceptualization (supporting); Investigation (supporting); Methodology (supporting); Validation (supporting). **Bin Gao:** Conceptualization (supporting); Investigation (equal); Methodology (equal); Resources (equal); Validation (equal). **Robert Vajtai:** Conceptualization (equal); Funding acquisition (equal); Investigation (equal); Methodology (equal); Project administration (equal); Resources (equal); Supervision (equal); Validation (equal); Writing – original draft (equal); Writing – review & editing (equal). **Pengcheng Dai:** Conceptualization (equal); Funding acquisition (equal); Investigation (equal); Project administration (equal); Supervision (equal); Validation (equal). **Pulickel M. Ajayan:** Conceptualization (equal); Funding acquisition (equal); Investigation (equal); Methodology (equal); Project administration (equal); Resources (equal); Supervision (equal); Validation (equal); Writing – original draft (equal); Writing – review & editing (equal). **Yuji Zhao:** Conceptualization (equal); Funding acquisition (equal); Investigation (equal); Methodology (equal); Project administration (equal); Resources (equal); Supervision (equal); Validation (equal); Writing – original draft (equal); Writing – review & editing (equal).

DATA AVAILABILITY

The data that support the findings of this study are available from the corresponding author upon reasonable request.

REFERENCES

[1]H. P. P. V. Shanmugasundram, E. Jayamani, and K. H. Soon, "A comprehensive review on dielectric composites: Classification of dielectric composites," Renew. Sustain. Energy Rev. **157**, 112075 (2022).

[2]M. Lokanathan, P. V. Acharya, A. Ouroua, S. M. Strank, R. E. Hebner, and V. Bahadur, "Review of nanocomposite dielectric materials with high thermal conductivity," Proc. IEEE **109**, 1364–1397 (2021).

[3]H. Li, H. Wang, Q. Tang, X. Lang, X. Wang, Y. Zong, and C. Zong, "Preparation of graphene/polypropylene composites with high dielectric constant and low dielectric loss via constructing a segregated graphene network," RSC Adv. **11**, 38264–38272 (2021).

[4]X. Pan, M. Wang, X. Qi, N. Zhang, T. Huang, J. Yang, and Y. Wang, "Fabrication of sandwich-structured PPy/MoS_2/PPy nanosheets for polymer composites with high dielectric constant, low loss and high breakdown strength," Compos. A: Appl. Sci. Manuf. **137**, 106032 (2020).

[5]A. Burke, "Prospects for the development of high energy density dielectric capacitors," Appl. Sci. **11**, 8063 (2021).

[6]X. Hao, "A review on the dielectric materials for high energy-storage application," J. Adv. Dielect. **3**, 1330001 (2013).

[7]S. J. Fiedziuszko, I. C. Hunter, T. Itoh, Y. Kobayashi, T. Nishikawa, S. N. Stitzer, and K. Wakino, "Dielectric materials, devices, and circuits," IEEE Trans. Microwave Theory Tech. **50**, 706–720 (2002).

[8]F. Hui, C. Pan, Y. Shi, Y. Ji, E. Grustan-Gutierrez, and M. Lanza, "On the use of two dimensional hexagonal boron nitride as dielectric," Microelectron. Eng. **163**, 119–133 (2016).

[9]J. Cao, T. L. Meng, X. Zhang, C. K. I. Tan, A. Suwardi, and H. Liu, "On functional boron nitride: Electronic structures and thermal properties," Mater. Today Electron. **2**, 100005 (2022).

[10]M. Xu, D. Wang, K. Fu, D. H. Mudiyanselage, H. Fu, and Y. Zhao, "A review of ultrawide bandgap materials: Properties, synthesis and devices," Oxf. Open Mater. Sci. **2**, itac004 (2022).

[11]Y. Ji, C. Pan, M. Zhang, S. Long, X. Lian, F. Miao, F. Hui, Y. Shi, L. Larcher, E. Wu, and M. Lanza, "Boron nitride as two dimensional dielectric: Reliability and dielectric breakdown," Appl. Phys. Lett. **108**, 012905 (2016).

[12]C. Cazorla and T. Gould, "Polymorphism of bulk boron nitride," Sci. Adv. **5**, eaau5832 (2019).

[13]K. Zhang, Y. Feng, F. Wang, Z. Yang, and J. Wang, "Two dimensional hexagonal boron nitride (2D-hBN): Synthesis, properties and applications," J. Mater. Chem. C **5**, 11992–12022 (2017).

[14]M. J. Molaei, M. Younas, and M. Rezakazemi, "A comprehensive review on recent advances in two-dimensional (2D) hexagonal boron nitride," ACS Appl. Electron. Mater. **3**, 5165–5187 (2021).

[15]A. Laturia, M. L. Van de Put, and W. G. Vandenberghe, "Dielectric properties of hexagonal boron nitride and transition metal dichalcogenides: From monolayer to bulk," npj 2D Mater. Appl. **2**, 6 (2018).

[16]P. B. Mirkarimi, K. F. McCarty, and D. L. Medlin, "Review of advances in cubic boron nitride film synthesis," Mater. Sci. Eng. R: Rep. **21**, 47–100 (1997).

[17]C. B. Samantaray and R. N. Singh, "Review of synthesis and properties of cubic boron nitride (c-BN) thin films," Int. Mater. Rev. **50**, 313–344 (2005).

[18]K. Chen, B. Song, N. K. Ravichandran, Q. Zheng, X. Chen, H. Lee, H. Sun, S. Li, G. A. G. U. Gamage, F. Tian, Z. Ding, Q. Song, A. Rai, H. Wu, P. Koirala, A. J. Schmidt, K. Watanabe, B. Lv, Z. Ren, L. Shi, D. G. Cahill, T. Taniguchi, D. Broido, and G. Chen, "Ultrahigh thermal conductivity in isotope-enriched cubic boron nitride," Science **367**, 555–559 (2020).

[19]M. Zhao, Z. Kou, Y. Zhang, B. Peng, Y. Wang, Z. Wang, X. Yin, M. Jiang, S. Guan, J. Zhang, and D. He, "Superhard transparent polycrystalline cubic boron nitride," Appl. Phys. Lett. **118**, 151901 (2021).

[20]M. E. Turiansky, D. Wickramaratne, J. L. Lyons, and C. G. Van de Walle, "Prospects for n-type conductivity in cubic boron nitride," Appl. Phys. Lett. **119**, 162105 (2021).

[21]Y. Yan, X. Fei, L. Huang, Y. Yu, Y. Wen, and G. Zhao, "Effect of BN content on the structural, mechanical, and dielectric properties of PDCs-SiCN(BN) composite ceramics," J. Am. Ceram. Soc. **106**, 6951–6961 (2023).

[22]S. Wang, D. Jia, Z. Yang, X. Duan, Z. Tian, and Y. Zhou, "Effect of BN content on microstructures, mechanical and dielectric properties of porous BN/Si_3N_4 composite ceramics prepared by gel casting," Ceram. Int. **39**, 4231–4237 (2013).

[23]T. Rampai, C. I. Lang, and I. Sigalas, "Investigation of MAX phase/c-BN composites," Ceram. Int. **39**, 4739–4748 (2013).

[24]S. Saha, A. Rice, A. Ghosh, S. M. N. Hasan, W. You, T. Ma, A. Hunter, L. J. Bissell, R. Bedford, M. Crawford, and S. Arafin, "Comprehensive characterization and analysis of hexagonal boron nitride on sapphire," AIP Adv. **11**, 055008 (2021).

[25]E. Guzman, F. Kargar, A. Patel, S. Vishwakarma, D. Wright, R. B. Wilson, D. J. Smith, R. J. Nemanich, and A. A. Balandin, "Optical and acoustic phonons in turbostratic and cubic boron nitride thin films on diamond substrates," Diam. Relat. Mater. **140**, 110452 (2023).

[26]A. Biswas, R. Xu, J. Christiansen-Salameh, E. Jeong, G. A. Alvarez, C. Li, A. B. Puthirath, B. Gao, A. Garg, T. Gray, H. Kannan, X. Zhang, J. Elkins, T. S. Pieshkov, R. Vajtai, A. G. Birdwell, M. R. Neupane, B. B. Pate, T. Ivanov, E. J. Garratt, P. Dai, H. Zhu, Z. Tian, and P. M. Ajayan, "Phase stability of hexagonal/cubic boron nitride nanocomposites," Nano Lett. **23**, 6927–6936 (2023).

[27]A. Biswas, M. Xu, K. Fu, J. Zhou, R. Xu, A. B. Puthirath, J. A. Hachtel, C. Li, S. A. Iyengar, H. Kannan, X. Zhang, T. Gray, R. Vajtai, A. G. Birdwell, M. R.

Neupane, D. A. Ruzmetov, P. B. Shah, T. Ivanov, H. Zhu, Y. Zhao, and P. M. Ajayan, "Properties and device performance of BN thin films grown on GaN by pulsed laser deposition," Appl. Phys. Lett. **121**, 092105 (2022).
[28]J. Ying, X. W. Zhang, Z. G. Yin, H. R. Tan, S. G. Zhang, and Y. M. Fan, "Electrical transport properties of the Si-doped cubic boron nitride thin films prepared by in situ cosputtering," J. Appl. Phys. **109**, 023716 (2011).
[29]S. S. Fouad, G. B. Sakr, I. S. Yahia, D. M. Abdel-Basset, and F. Yakuphanoglu, "Capacitance and conductance characterization of nano-$ZnGa_2Te_4$/n-Si diode," Mater. Res. Bull. **49**, 369–383 (2014).
[30]V. Khopkar and B. Sahoo, "Low temperature dielectric properties and NTCR behavior of the $BaFe_{0.5}Nb_{0.5}O_3$ double perovskite ceramic," Phys. Chem. Chem. Phys. **22**, 2986–2998 (2020).
[31]A. M. Akbaş, A. Tataroğlu, Ş. Altındal, and Y. Azizian-Kalandaragh, "Frequency dependence of the dielectric properties of Au/(NG: PVP)/n-Si structures," J. Mater. Sci.: Mater. Electron. **32**, 7657–7670 (2021).
[32]S. Hong, C.-S. Lee, M.-H. Lee, Y. Lee, K. Y. Ma, G. Kim, S. I. Yoon, K. Ihm, K.-J. Kim, T. J. Shin, S. W. Kim, E.-c. Jeon, H. Jeon, J.-Y. Kim, H.-I. Lee, Z. Lee, A. Antidormi, S. Roche, M. Chhowalla, H.-J. Shin, and H. S. Shin, "Ultralow-dielectric-constant amorphous boron nitride," Nature **582**, 511–514 (2020).
[33]Y. Huang, J. Ji, Y. Chen, X. Li, J. He, X. Cheng, S. He, Y. Liu, and J. Liu, "Broadband microwave absorption of $Fe_3O_4BaTiO_3$ composites enhanced by interfacial polarization and impedance matching," Compos. B: Eng. **163**, 598–605 (2019).
[34]W. Wan, J. Luo, C. Huang, J. Yang, Y. Feng, W. Yuan, Y. Ouyang, D. Chen, and T. Qiu, "Calcium copper titanate/polyurethane composite films with high dielectric constant, low dielectric loss and super flexibility," Ceram. Int. **44**, 5086–5092 (2018).
[35]M. P. F. Graça, A. Meireles, C. Nico, and M. A. Valente, "Nb_2O_5 nanosize powders prepared by sol–gel–structure, morphology and dielectric properties," J. Alloys Compd. **553**, 177–182 (2013).
[36]R. Zhang, L. Gao, H. Wang, and J. Guo, "Dielectric properties and space charge behavior in ceramic capacitor," Appl. Phys. Lett. **85**, 2047–2049 (2004).
[37]A. Biswas, G. A. Alvarez, M. Tripathi, J. Lee, T. S. Pieshkov, C. Li, B. Gao, A. B. Puthirath, X. Zhang, T. Gray, J. Elkins, R. Vajtai, P. Dai, A. G. Birdwell, M. R. Neupane, T. Ivanov, E. J. Garratt, B. B. Pate, A. K. Roy, A. Dalton, Z. Tian, and P. M. Ajayan, "Cubic and hexagonal boron nitride phases and phase boundaries," J. Mater. Chem. C **12**, 3053–3062 (2024).
[38]G. Wu, Y. Cheng, Z. Yang, Z. Jia, H. Wu, L. Yang, H. Li, P. Guo, and H. Lv, "Design of carbon sphere/magnetic quantum dots with tunable phase compositions and boost dielectric loss behavior," Chem. Eng. J. **333**, 519–528 (2018).
[39]C. J. Anjeline, D. P. Mali, and N. Lakshminarasimhan, "High dielectric constant of $NiFe_2O_4$–$LaFeO_3$ nanocomposite: Interfacial conduction and dielectric loss," Ceram. Int. **47**, 34278–34288 (2021).